Biochemical Pharmacology 81 (2011) 1228–1236

Contents lists available at ScienceDirect

Biochemical Pharmacology

journal homepage: www.elsevier.com/locate/biochempharm

MG132 treatment attenuates cardiac remodeling and dysfunction following aortic banding in rats via the NF-κB/TGFβ1 pathway

Yuedong Ma [a], Baolin Chen [b], Dan Liu [a], Yang Yang [c], Zhaojun Xiong [d], Junyi Zeng [a], Yugang Dong [a,e,*]

[a] Department of Cardiology, The First Affiliated Hospital of Sun Yat-Sen University, Guangzhou 510080, PR China
[b] Department of Cardiology, The People's Hospital of Guizhou Province, Guiyang 550002, PR China
[c] Department of Pathology, The First Affiliated Hospital of Sun Yat-Sen University, Guangzhou 510080, PR China
[d] Department of Cardiology, The Third Affiliated Hospital of Sun Yat-Sen University, Guangzhou 510080, PR China
[e] Key Laboratory on Assisted Circulation, Ministry of Health, Guangzhou 510080, PR China

ARTICLE INFO

Article history:
Received 31 January 2011
Accepted 9 March 2011
Available online 21 March 2011

Keywords:
Pressure overload
Proteasome inhibition
Cardiac remodeling
Heart failure
NF-κB

ABSTRACT

Although MG132, a proteasome inhibitor, is suggested to impede secondary cardiac remodeling after hypertension, the mechanism and optimal duration of treatment remain unknown. This study was designed to investigate the effects and possible mechanism of MG132 on hypertension-induced cardiac remodeling. Male Sprague–Dawley rats subjected to abdominal aortic constriction (AAC) or sham operation received an intraperitoneal injection of MG132 (0.1 mg kg^{-1} day^{-1}) or vehicle over a 2- or 8-week period. In the end, left ventricular (LV) function was evaluated with echocardiography and pressure tracing. Collagen deposition within the LV myocardium was assessed with Masson's trichrome staining. Ubiquitin-proteasome system (UPS), NF-κB, I-κB, TGFβ1 and Smad2 within the LV tissue were evaluated. In addition, angiotensin II within both plasma and LV tissue was also examined. Compared with the sham groups, the vehicle-treated AAC group exhibited a higher angiotensin II level, LV/body weight ratio, septal and posterior wall thicknesses, and a markedly reduced cardiac function ($P < 0.05$). Treatment with MG132 for 8 weeks attenuated these cardiac remodeling parameters and improved cardiac function ($P < 0.01$). 2- and 8-week hypertension led to activation of UPS, which was followed by activation of NF-κB and increased expression of TGFβ1 and Smad2 ($P < 0.01$). MG132 significantly inhibited NF-κB activity and down-regulate the levels of TGFβ1 and Smad2 expression by 2 and still at 8 weeks ($P < 0.01$). Short- and long-term treatment with MG132 significantly attenuated hypertension-induced cardiac remodeling and dysfunction, which may be mediated by the NF-κB/TGFβ1 signaling pathway.

1. Introduction

Hypertension in adults is a common disease, which often leads to gradual dysfunction of vital organs, such as heart, brain and kidney. In heart, incessant fibrosis within the myocardium due to fibroblast proliferation and deposition of collagen plays a key role in the transition from initial cardiomyocyte hypertrophy to later cardiac remodeling, the result of which is heart failure [1,2]. Therefore, prevention of myocardial remodeling secondary to uncontrollable long-term hypertension can theoretically interrupt the progression towards heart failure. Various antihypertensive medications including angiotensin-converting enzyme inhibitors, angiotensin II receptor blockers, and β-blockers have been widely used in clinic, yet the incidence of heart failure and resulting mortality remain high [3]. It is necessary to search for new medications capable of impeding the progression of fibrosis despite long-term exposure of the left ventricle (LV) to high blood pressure.

Recent studies have paid increasing attention to the relationship between the ubiquitin-proteasome system (UPS) and development of cardiac remodeling. The available data regarding their relationship, however, are highly variable across different laboratories. For example, some groups have reported that proteasome activity within the myocardial tissue is depressed

Abbreviations: AAC, abdominal aortic constriction; TAC, transverse aortic constriction; LV, left ventricle; UPS, ubiquitin-proteasome system; CHF, congestive heart failure; Ang II, angiotensin II; MAPK, mitogen-activated protein kinase; BW, body weight; LVW, left ventricular weight; LV/BW, left ventricular/body weight ratio; Lung/BW, lung/body weight ratio; HR, heart rate; LVSP, left ventricular systolic pressure; LVEDP, left ventricular end-diastolic pressure; +dP/dtmax, the maximal rate of LV contraction; −dP/dtmax, the maximal rate of LV relaxation; IVSd, interventricular septal thickness; PWd, left ventricular posterior wall thickness; LVDd, left ventricular end-diastolic diameter; FS, fractional shortening; EF, ejection fraction.

* Corresponding author at: Department of Cardiology, The First Affiliated Hospital of Sun Yat-Sen University, 58 Zhongshan II Road, Guangzhou 510080, PR China. Tel.: +86 20 87332200 8151; fax: +86 20 87332200 8151.
E-mail address: doctormayuedong@yahoo.com.cn (Y. Dong).

0006-2952/$ – see front matter © 2011 Elsevier Inc. All rights reserved.
doi:10.1016/j.bcp.2011.03.009

during the development of cardiac hypertrophy, and subsequent remodeling is induced by the pressure overload [4–7]. Progression towards congestive heart failure (CHF) results from impaired removal of abnormal proteins by proteasome as a result of dysfunction of proteasome activity, which has been observed during the transition process from compensated cardiac hypertrophy to CHF [6]. In contrast, other groups gradually revealed that, during hypertension, the proteasome played an active role in the development of cardiomyocyte hypertrophy [8–10]. Inhibition of proteasome activity has been suggested as beneficial for the prevention of cardiac hypertrophy [8,11]. Some studies showed that there were several signal pathways (Akt, calcineurin/NFAT) that could be down-regulated in response to proteasome inhibition [12,13]. Our previous study has also shown that MG132 could attenuate cardiac hypertrophy resulting from pressure overload mainly through MAPKs signaling pathways [14]. However, these studies mainly focused on hypertrophy in cardiomyocytes, whereas cardiac fibrosis and remodeling received much less attention. A recent study suggested that treatment of spontaneously hypertensive rats with MG132, a well-characterized proteasome inhibitor, may be helpful to prevent cardiac fibrosis as it could suppress the expression of matrix metalloproteinases and collagens, however, the effect of prevention of cardiomyocyte hypertrophy or ventricular remodeling with MG132 was not evaluated [15].

Before this strategy can be successfully transferred to clinical use, several important questions must be addressed. For example, is activation of UPS a prerequisite for cardiac remodeling during hypertension? If so, does its activation continue throughout the entire process of cardiac remodeling? Can such remodeling be prevented by short- or long-term administration of MG132 and is there any other signaling pathway underlying these effects?

Numerous studies have suggested that the transforming growth factor beta 1 (TGF-β1)/Smads signaling pathways play a very important role in cardiac fibrosis and remodeling [16–19]. It is well-established that TGF-β1 is capable of regulating several important cellular processes such as proliferation, differentiation, migration and apoptosis mainly through the Smads signaling pathway [20]. In addition, recent studies have revealed that NF-κB, an inflammation-related transcription factor, is responsible for the regulation of TGF-β1 expression [21,22]. It has also been suggested that UPS is indispensable for the activation of NF-κB through a proteasome-mediated degradation of I-κB [23,24].

Therefore, we hypothesized that, via indirect inhibition of NF-κB, administration of MG132 will inhibit cardiac fibrosis under conditions of hypertension. In the present study, a surgically-induced model of rat hypertension was employed to determine the efficiency and mechanism of short- and long-term exposure of rat heart to MG132 for the prevention of secondary cardiac remodeling.

2. Methods

All protocols were approved by the Institutional Animal Care and Use Committee. In addition, investigations were carried out according to the Guide for Care and Use of Laboratory Animals published by the US National Institute of Health (NIH Publication No. 85-23, revised 1996).

2.1. Animal models and experimental designs

Male Sprague–Dawley rats (6 weeks old; body weight 150–200 g) were obtained from the animal service center at our institution. All animals were housed in individual cages on a 12 h light–dark cycle in a room with temperature (~24 °C) and humidity control, and with *ad libitum* access to tap water and standard rodent chow. After anesthesia by intraperitoneal injection of pentobarbital (50 mg kg^{-1}), a midline abdominal incision was made to expose the aorta. The aorta was isolated above the renal arteries, and a 21-gauge needle was placed alongside it. Then, both the aorta and the needle were securely tied together using a 4-0 suture. After the needle was quickly retracted away, abdominal aortic constriction (AAC) with 70–80% reduction of lumen diameter (~0.8 mm of outer aortic diameter) was established. Similar surgery was performed on the sham-operated rats, with the exception of the aortic banding procedure.

Three days after operation, all surviving rats received an intraperitoneal injection of either MG132 (0.1 mg kg^{-1}, ALEXIS, San Diego, CA) or solvent alone (0.1% DMSO) once a day for a duration of 2 or 8 weeks. Thus, the study cohort was composed of four groups: (1) MG132/Sham; (2) Vehicle/Sham; (3) MG132/AAC; and (4) Vehicle/AAC. Each group included two subgroups: 2 and 8 weeks (n = 15, per subgroup). In the present study, the rat survival rate 3 days following the AAC operation was 80%.

MG132 (N-[(phenylmethoxy)-carbonyl]-L-leucyl-N-[(1S)-1-formyl-3-methylbutyl]-L-leucinamide) is a specific, potent, reversible, and cell-permeable proteasome inhibitor (K_i = 4 nM) [25]. It plays a key role in blocking the degradation of ubiquitin-conjugated proteins in mammalian cells and permeable strains of yeast by the 26S complex without affecting its ATPase or isopeptidase activities. MG132 can inhibit NF-κB activation by reducing the degradation of IκB-α.

The dose of MG-132 used in the present experiment was determined on the basis of previous studies [14,15] and our preliminary experiments evaluating the effects and side effects of different doses of MG132 on rats by detecting laboratory markers that indicate renal or hepatic function (data not shown). 0.1 mg kg^{-1} day^{-1} for 2 or 8 weeks is a rather low dose-intensity, but effectively prevented cardiac remodeling and dysfunction in pressure-overloaded hearts without marked drug toxicity.

2.2. Measurements

2.2.1. Doppler echocardiography and hemodynamics

Two or eight weeks after the treatment, each rat was weighed again. The same anesthetization procedure as before was carried out, and transthoracic echocardiography (ATL-HDI5000, equipped with a 10-MHz transducer) was performed for each rat. Measurements were obtained for the left ventricular end-diastolic diameter, septal and posterior wall thicknesses, fractional shortening and ejection fraction. All measurements were performed by an experienced technologist who was blinded to study groups and averaged over 10 consecutive cardiac cycles.

A catheter was introduced through the right carotid artery into the left ventricle for hemodynamic measurements in all animals. Then, heart rate, carotid artery pressure, LV systolic pressure, LV end-diastolic pressure, the maximal rate of LV contraction (+dP/dtmax) and the maximal rate of LV relaxation (−dP/dtmax) were measured with a commercially available analog-to-digital converter (RX104A, Biopic, Goleta, CA, USA) and analyzed with BIOPAC software (Goleta, CA, USA).

2.2.2. Proteasome activity

Proteasome activity was measured using the peptide substrates Succinyl-Leu-Leu-Val-Tyr-7-amino-4-methylcoumarin (SLLVY-AMC), Benzoylcarbonyl-Leu-Leu-Gly-AMC (Z-LLE-AMC), and Benzoyl-Val-Gly-Arg-AMC (Bz-VGR-AMC) (Astra Merck Inc., Wayne, PA, USA). The tissue from the left ventricular free wall of all survived rats after 24 h following the last administration with MG132 was homogenized using a polytron in lysis buffer (50 mM HEPES, 5 mM EDTA, 150 mM NaCl, 1% Triton X-100), then centrifuged at 400 × g for 15 min at 4 °C. The activities of

chymotrypsin-like, caspase-like, and trypsin-like peptidases of proteasome were detected using their respective substrates, according to the method reported previously [26–29]. Briefly, 20 μg protein homogenate mixed with 25 mM Tris–HCl, pH 7.0, and 40 μM proteasome peptidase substrates in total volume of 150 μL was incubated for 1 h at 37 °C. The reaction was terminated by addition of 150 μL of ice-cold 96% (vol./vol.) ethanol. Subsequently, the fluorescence of each solution was monitored by detecting the release of AMC with spectrophotometry (HitachF-2000; Hitachi Instruments, Tokyo, Japan) at an excitation wavelength of 380 nm and an emission wavelength of 440 nm. All results were standardized by the fluorescence intensity of an equal volume of free AMC (Sigma, St. Louis, MO, USA).

2.2.3. Angiotensin II levels

Two or eight weeks after treatment, measurement of angiotensin II was carried out using commercially available kits. Before each rat was sacrificed, 5 mL of blood was collected from the right carotid artery. The blood samples were centrifuged at 170 × *g* for 5 min at 4 °C. The plasma was collected immediately and stored at −30 °C until use. Left ventricular samples were used to measure tissue concentration of angiotensin II. After being immersed in 1 mL of normal saline containing 25 μL of dimercaprol (0.32 M), 50 μL of EDTA–Na2 (0.30 M) and 50 μL of 8-hydroxyquinoline (0.34 M), each tissue sample (100 mg) was mechanically homogenized on ice. The homogenates were then centrifuged at 250 × *g* for 15 min at 4 °C. The supernatant was collected and stored at −30 °C. The levels of angiotensin II in plasma and tissue were measured by radioimmunoassay (Northern Biot Co, Beijing, China) according to the manufacturer's instructions. The intra-assay variation was determined to be <5%, and the inter-assay variation was <10%.

2.2.4. Tissue collagen ratio

Hearts were arrested at diastole with an intraventricular injection of KCl solution (30 mM). Hearts and lungs were excised, washed with PBS, and dried with filter paper. Then, the lung, heart and LV were separated and weighed. Left ventricular samples were snap frozen in liquid nitrogen and either stored at −80 °C or fixed with 10% phosphate-buffered formalin. Frozen tissue samples were subsequently used for real-time quantitative PCR and western blot assay. Fixed tissue samples were embedded in paraffin, cut into 4 μm sections and stained with Masson's trichrome to detect collagen (blue) and cardiomyocytes (red). Each slice of heart includes whole LV which can be divided into four parts (four walls of the LV). Two sections were then cut from each part, and 4 radially oriented microscopic fields were selected at random from each section at a magnification of 100×. The percentage of the area occupied by collagen was quantitated using an analysis software package (Image Pro-Plus 5.5). The percentage of perivascular collagen was calculated as the sum of vascular collagen-positive areas divided by the sum of vessel areas. Percentage of interstitial collagen was calculated as the sum of all non-vascular collagen-positive areas divided by the sum of the total tissue area excluding the vessel area from the region of interest.

2.2.5. NF-κB activity assay

Nuclear protein extraction was achieved from part of the frozen tissue by means of a Nuclear Extraction kit (Cayman Chemicals, Ann Arbor, MI, USA), according to the manufacturer's instructions. After, the activity of NF-κB was measured with enzyme-linked immunosorbent assay (ELISA) via an NF-κB (p65) transcription factor assay kit from the same company, according to the manufacturer's protocol.

2.2.6. Real-time reverse transcription-PCR

Total RNA was extracted from the frozen LV tissue with Trizol reagent (Invitrogen, Carlsbad, CA, USA), according to the manufacturer's protocol, in order to evaluate the transcriptional levels of ubiquitin and TGF-β1, respectively. Firstly, cDNA synthesis was performed from total RNA using MMLV reverse transcriptase (Takara, Japan). Secondly, real-time quantitative PCR was performed for rat ubiquitin, TGF-β1 and GAPDH (control) using an ABI 9700 sequencer (Applied Biosystems, Foster City, CA, USA). The primers' sequences were as follows: rat ubiquitin, 5′-ACTCGTACCTTTCTCACCA-3′ and 5′-AACTAAGACACCTCCCCTA-3′; rat TGF-β1, 5′-CAAGGAGACGGAATACAGGG-3′ and 5′-TGAGGAGCAGGAAGGGTC-3′; rat GAPDH, 5′-TGGTCTACATGTTCCAGTATGACT-3′ and 5′-CCATTTGATGTTAGCGGGATCTC-3′. The reactions were carried out in the following conditions: denaturation at 94 °C for 30 s; annealing at 58 °C for 30 s; and, extension at 72 °C for 30 s.

2.2.7. Western blotting

Cardiac tissues were homogenized in liquid nitrogen and then in SDS sample buffer to extract proteins. Total protein concentration was determined using the BCA Protein Assay Kit (Santa Cruz Biotechnology, Santa Cruz, CA, USA). 30 μg of total protein from the LV tissue was then loaded to a 10% or 12% SDS–polyacrylamide gel and electroblotted to a PVDF membrane. The membrane was blocked for 2 h at room temperature in blocking solutions and incubated with primary antibodies anti-TGF-β1 (1:500 dilution; Santa Cruz Biotechnology, Santa Cruz, CA, USA), anti-Smad2 (1:1000; Cell Signaling Inc., Beverly, MA, USA), anti-NF-κB (p65) (1:1000; Santa Cruz Biotechnology), anti-IκB-α (1:2000; Santa Cruz Biotechnology) and anti-GAPDH (1:40,000; Boshide Inc., Wuhan, China) and then washed with TBS-T (10 mM Tris–HCl, pH 8.0, 150 mM NaCl, and 0.1% Tween 20). After washing, the membranes were incubated with anti-mouse or rat IgG secondary antibody (Boshide Inc.) at 37 °C for 1 h, and the immune complex was detected with enhanced chemiluminescence (Millipore, Beyotime Inc., Jiangsu, China) that was quantified by densitometry.

2.2.8. Immunofluorescence analysis

To investigate the expression levels of total ubiquitin protein, including free ubiquitin and ubiquitin binding with the target proteins we conducted immunofluorescent examination with a mouse anti-ubiquitin antibody (Sigma). Immunofluorescence assay was performed using an immunodetection kit (Boster Inc., Wuhan, China), according to the manufacturer's protocol.

2.3. Statistical analyses

The data were expressed as mean ± SE. One-way ANOVA and subsequent Student–Newman–Keuls test were used for comparison of differences in variables with normal distribution between the groups. A value of <0.05 was considered statistically significant. Statistical analyses were performed using SPSS 10.0 software (SPSS Inc., Chicago, IL, USA).

3. Results

A total of 46 rats survived in the 2 week subgroups: 12 rats in the Vehicle/Sham group; 11 rats in the MG132/Sham group; 11 rats in the Vehicle/AAC group; and 12 rats in the MG132/AAC group. Forty-one rats survived in the 8-week subgroups: 11 rats in the Vehicle/Sham group; 10 rats in the MG132/Sham group; 10 rats in the Vehicle/AAC group; and 10 rats in the MG132/AAC group.

Table 1
Effects of 2 weeks' treatment with MG132 on echocardiography and hemodynamic measurements.

Parameters	Vehicle/Sham ($n=12$)	MG132/Sham ($n=11$)	Vehicle/AAC ($n=11$)	MG132/AAC ($n=12$)
HR (beats/min)	364.75 ± 7.37	375.91 ± 15.71	416.45 ± 13.64	378.75 ± 8.70
LVSP (mmHg)	114.62 ± 3.07	115.98 ± 3.21	143.08 ± 1.42##	138.82 ± 1.42##
LVEDP (mmHg)	3.81 ± 0.17	3.66 ± 0.71	10.00 ± 0.21##	6.11 ± 0.26##,**
+dP/dtmax (mmHg/ms)	5.91 ± 0.24	5.84 ± 0.28	3.52 ± 0.18##	3.63 ± 0.14##
−dP/dtmax (mmHg/ms)	5.36 ± 0.11	5.29 ± 0.31	3.31 ± 0.15##	4.68 ± 0.13#,**
IVSd (mm)	1.88 ± 0.04	1.84 ± 0.02	2.25 ± 0.11##	1.86 ± 0.05**
PWd (mm)	1.80 ± 0.02	1.86 ± 0.02	2.03 ± 0.06##	1.90 ± 0.04#,*
LVDd (mm)	4.25 ± 0.17	4.19 ± 0.13	4.67 ± 0.11#	4.46 ± 0.16#
FS (%)	43.61 ± 1.01	42.34 ± 1.06	38.15 ± 1.09##	38.46 ± 1.57##
EF (%)	82.98 ± 1.17	83.90 ± 0.88	64.05 ± 3.70##	68.39 ± 2.58##

HR: heart rate, LVSP: left ventricular systolic pressure, LVEDP: left ventricular end-diastolic pressure, +dP/dtmax: the maximal rate of LV contraction, −dP/dtmax: the maximal rate of LV relaxation, IVSd: interventricular septal thickness, PWd: left ventricular posterior wall thickness, LVDd: left ventricular end-diastolic diameter, FS: fractional shortening, EF: ejection fraction.
# $P<0.05$ *vs.* vehicle-treated sham group.
$P<0.01$ *vs.* vehicle-treated sham group.
* $P<0.05$ *vs.* vehicle-treated AAC group.
** $P<0.01$ *vs.* vehicle-treated AAC group.

3.1. Echocardiography

As shown in Table 1 and Fig. 1, 2 weeks of hypertension led to increase in LV end-diastolic diameter as well as septal and posterior wall thicknesses for rats lacking MG132 treatment (Vehicle/AAC group). Fractional shortenings were also found to be significantly impaired in these rats. Use of MG132 (MG132/AAC group) not only reduced such changes in septal and posterior wall thickness but also improved cardiac diastolic function.

As shown in Table 2 and Fig. 1, 8 weeks of hypertension led to similar echocardiographical changes as was seen in the 2-week Vehicle/AAC subgroup. However, use of MG132 for 8 weeks significantly reduced such impairment in LV end-diastolic diameter, fractional shortening, and ejection fraction ($P<0.01$).

Echocardiographic data indicated long-term treatment with MG132 also significantly attenuated heart systolic dysfunction, although this phenomenon was not observed in the 2-week subgroup.

3.2. Hemodynamic measurements

As shown in Table 1, 2 weeks of hypertension led to increases in LV systolic pressure and end-diastolic pressure, as well as reductions in +dP/dtmax and −dP/dtmax in rats from the Vehicle/AAC group, as compared with those in the Vehicle/Sham group. MG132 treatment only led to reduced impairment in LV end-diastolic pressure and −dP/dtmax ($P<0.01$).

As shown in Table 2, 8 weeks of AAC led to similar changes as observed after only 2 weeks of hypertension. In contrast, long-term MG132 treatment in rats with AAC led to more significant protection in LV end-diastolic pressure, −dP/dtmax and +dP/dtmax, as compared to those rats not treated with MG132 ($P<0.01$).

3.3. Cardiac morphometric parameters, total collagen and angiotensin II

As shown in Table 3, rats in the 2-week subgroups exhibited no differences among their lung/body weight ratios. The LV weight (LVW), LV/body weight ratio (LV/BW), perivascular and interstitial collagen volume fraction, plasma and myocardium angiotensin II levels in the Vehicle/AAC group significantly increased, as compared to those parameters in the Vehicle/Sham group. MG132 treatment prevented or alleviated the increase in LVW, LV/BW, perivascular and interstitial collagen volume fraction as compared to the Vehicle/AAC group. These parameters, however, were not found to be significantly different between the Vehicle/Sham group and the MG132/Sham group.

At 8 weeks following AAC, administration of MG132 exhibited decreased hypertrophic responses as well as cardiac remodeling, in

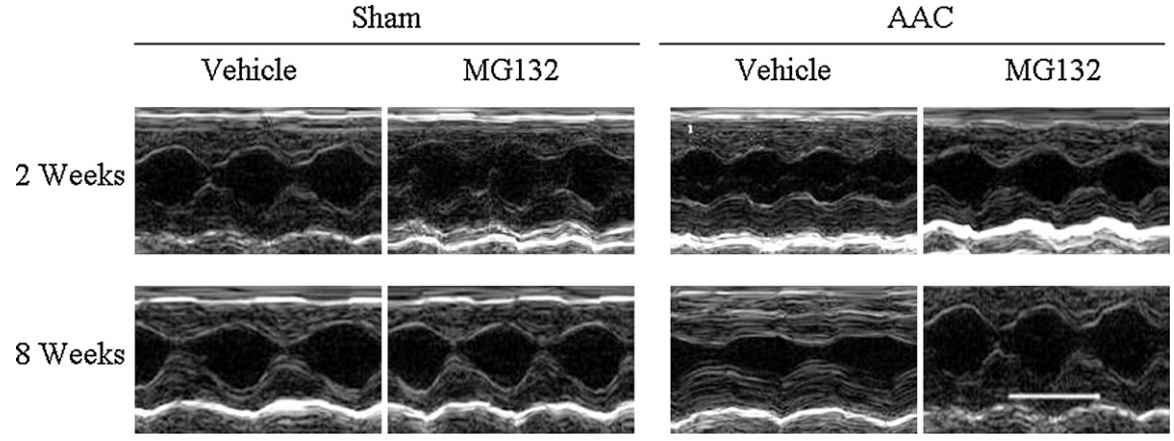

Fig. 1. Representative echocardiograms. Treatment with MG132 for 2 weeks significantly attenuated cardiac remodeling and diastolic dysfunction due to pressure overload as indicated by reduced LV end-diastolic diameter, septal and posterior wall thicknesses and increased maximal rate of LV relaxation ($P<0.05$), 8 weeks' treatment with MG132 not only alleviated cardiac remodeling but also improved cardiac systolic function as reflected by an increase in the maximal rate of LV contraction, fractional shortening, and ejection fraction ($P<0.01$). Bar, 10 mm.

Table 2
Effects of 8 weeks' treatment with MG132 on echocardiography and hemodynamic measurements.

Parameters	Vehicle/Sham ($n=11$)	MG132/Sham ($n=10$)	Vehicle/AAC ($n=10$)	MG132/AAC ($n=10$)
HR (beats/min)	399.73 ± 4.86	396.20 ± 5.41	405.20 ± 6.22	403.90 ± 10.35
LVSP (mmHg)	112.45 ± 3.05	108.82 ± 3.31	164.40 ± 2.05##	163.57 ± 1.57##
LVEDP (mmHg)	4.02 ± 0.18	4.33 ± 0.19	12.45 ± 0.60##	5.24 ± 0.23#,**
+dP/dtmax (mmHg/ms)	5.59 ± 0.17	5.23 ± 0.26	3.23 ± 0.23##	5.21 ± 0.24**
−dP/dtmax (mmHg/ms)	5.30 ± 0.19	4.98 ± 0.09	2.96 ± 0.19##	4.90 ± 0.23**
IVSd (mm)	2.08 ± 0.02	1.93 ± 0.02	3.01 ± 0.10##	2.05 ± 0.03**
PWd (mm)	1.85 ± 0.02	1.86 ± 0.04	2.76 ± 0.11##	2.01 ± 0.03**
LVDd (mm)	4.75 ± 0.11	4.65 ± 0.21	6.26 ± 0.15##	5.06 ± 0.06**
FS (%)	44.53 ± 1.35	42.81 ± 1.16	35.77 ± 1.40##	43.73 ± 0.93**
EF (%)	83.41 ± 1.06	84.49 ± 1.28	48.26 ± 2.38##	71.22 ± 1.88##,**

HR: heart rate, LVSP: left ventricular systolic pressure, LVEDP: left ventricular end-diastolic pressure, +dP/dtmax: the maximal rate of LV contraction, −dP/dtmax: the maximal rate of LV relaxation, IVSd: interventricular septal thickness, PWd: left ventricular posterior wall thickness, LVDd: left ventricular end-diastolic diameter, FS: fractional shortening, EF: ejection fraction.
# $P<0.05$ *vs.* vehicle-treated sham group.
$P<0.01$ *vs.* vehicle-treated sham group.
** $P<0.01$ *vs.* vehicle-treated AAC group.

terms of LVW, LV/BW ratio, LW/BW ratio, and perivascular and interstitial collagen volume fraction (Tables 3 and 4). Therefore, our data supported the effect that MG132 could prevent cardiac hypertrophy and remodeling following pressure overload.

3.4. Ubiquitin and TGFβ1 expression

As shown in Fig. 2, ubiquitin and TGFβ1 mRNA expression were found to be significantly higher in the Vehicle/AAC group (at both 2 and 8 weeks), as compared to the Vehicle/Sham group ($P<0.01$). Both short- and long-term administration of MG132 reduced the enhanced transcription of TGFβ1, whereas it did not significantly influence that of ubiquitin; although the level of ubiquitin mRNA expression specifically at 8 weeks was not notably higher in the MG132/AAC group than the Vehicle/AAC group.

Expression of ubiquitin protein is shown in Fig. 3; its level was observed to increase significantly in the Vehicle/AAC group when compared with the Vehicle/Sham group ($P<0.01$). Treatment with MG132 for 2 or 8 weeks did not detectably increase its levels ($P>0.05$), although the level of ubiquitin protein expression at 8 weeks was not significantly higher.

3.5. Proteasome activity

As shown in Fig. 4, the chymotrypsin-like, trypsin-like, and caspase-like activities of proteasome increased significantly in the Vehicle/AAC group, as compared to the Vehicle/Sham group, both after 2 and 8 weeks. Administration of MG132 significantly inhibited the proteasome activity in rats with or without aortic constriction.

3.6. NF-κB activity

As shown in Fig. 5, NF-κB activity significantly increased in the Vehicle/AAC group, as compared to the Vehicle/Sham group ($P<0.01$), for both the 2- and 8-week time points. Treatment with MG132 attenuated the increased activity of NF-κB ($P<0.01$).

3.7. Effects of MG132 on NF-κB signaling pathways

To further elucidate the protective mechanisms of MG132 on the rat heart, we measured the levels of several proteins involved in the NF-κB signaling pathway.

Significantly elevated expression was detected for NF-κB (p65), TGFβ1 and Smad2, with a concomitant depression of IκB-α, in the Vehicle/AAC group, as compared to the Vehicle/Sham group ($P<0.01$; Fig. 6). Treatment with MG132 reduced the extent of this change.

Interestingly, we found in the present study that MG132 treatment had no significant effect on IκB-α expression in the heart of sham-operated rats (Fig. 6), although proteasome activity in these rats was markedly reduced (Fig. 4).

4. Discussion

Although multiple studies have addressed the role of UPS in the acute phase of LVH that follows transverse aortic constriction, the effects and mechanisms of UPS on the prevention of cardiac fibrosis, left ventricular remodeling and chronic heart failure remain largely unknown.

In the present study, we utilized a rat AAC model to determine the short- and long-term effects of the proteasome inhibition on the pressure overload heart. The AAC procedure in rat or TAC (transverse aortic constriction) in mouse is commonly used to produce pressure overload [30,31]. These two constriction models have similar mechanisms and effects on cardiac remodeling and heart failure. Although the likelihood of hypertrophy and cardiac dysfunction seemed to be higher as the band was placed closer to the heart, the AAC rat model with mild effects on the heart is more

Table 3
Effects of 2 weeks' treatment with MG132 on cardiac morphometric parameters and collagen content.

Parameters	Vehicle/Sham ($n=12$)	MG132/Sham ($n=11$)	Vehicle/AAC ($n=11$)	MG132/AAC ($n=12$)
BW (g)	245.00 ± 13.79	246.00 ± 12.32	216.45 ± 23.21	223.33 ± 18.74
LVW (g)	0.51 ± 0.08	0.59 ± 0.07	0.72 ± 0.15##	0.53 ± 0.13**
LV/BW (mg/g)	2.16 ± 0.25	2.40 ± 0.22	3.35 ± 0.57##	2.48 ± 0.51**
Lung/BW (mg/g)	6.38 ± 0.78	6.30 ± 0.85	7.36 ± 1.39	6.54 ± 1.60
Perivascular collagen (%)	10.63 ± 1.82	10.49 ± 2.54	40.49 ± 9.46##	23.19 ± 6.98##,**
Interstitial collagen (%)	3.25 ± 1.11	3.87 ± 0.78	4.16 ± 1.19##	3.28 ± 0.82**
Plasma Ang II (ng/L)	755.50 ± 164.78	863.19 ± 144.72	1524.6 ± 284.1##	1386.6 ± 250.88##
Myocardial Ang II (pg/L)	461.15 ± 114.26	445.53 ± 141.03	940.1 ± 126.70##	909.8 ± 124.47##

BW: body weight, LVW: left ventricular weight, LV/BW: left ventricular/body weight ratio, Lung/BW: lung/body weight ratio.
$P<0.01$ *vs.* vehicle-treated sham group.
** $P<0.01$ *vs.* vehicle-treated AAC group.

Table 4
Effects of 8 weeks' treatment with MG132 on cardiac morphometric parameters and collagen content.

Parameters	Vehicle/Sham ($n=11$)	MG132/Sham ($n=10$)	Vehicle/AAC ($n=10$)	MG132/AAC ($n=10$)
BW (g)	346.36 ± 15.03	350.00 ± 5.96	337.00 ± 16.87	328.60 ± 5.48
LVW (g)	0.71 ± 0.05	0.75 ± 0.04	1.01 ± 0.07$^{\#\#}$	0.80 ± 0.04**
LV/BW (mg/g)	2.02 ± 0.09	2.14 ± 0.09	3.04 ± 0.25$^{\#\#}$	2.45 ± 0.10$^{\#,**}$
Lung/BW (mg/g)	5.90 ± 0.44	5.64 ± 0.12	11.61 ± 0.79$^{\#\#}$	7.20 ± 0.25**
Perivascular collagen (%)	15.72 ± 1.31	13.77 ± 1.07	75.40 ± 2.10$^{\#\#}$	24.02 ± 2.32$^{\#\#,**}$
Interstitial collagen (%)	4.80 ± 0.51	3.47 ± 0.24	16.14 ± 1.24$^{\#\#}$	3.13 ± 0.26**
Plasma Ang II (ng/L)	1100.30 ± 76.70	1079.50 ± 68.77	2071.70 ± 57.59$^{\#\#}$	1941.10 ± 81.14$^{\#\#}$
Myocardium Ang II (pg/L)	584.39 ± 46.69	557.06 ± 37.62	890.53 ± 59.11$^{\#\#}$	915.37 ± 43.19$^{\#\#}$

BW: body weight, LVW: left ventricular weight, LV/BW: left ventricular/body weight ratio, Lung/BW: lung/body weight ratio.
$^{\#}$ $P<0.05$ *vs.* vehicle-treated sham group.
$^{\#\#}$ $P<0.01$ *vs.* vehicle-treated sham group.
** $P<0.01$ *vs.* vehicle-treated AAC group.

suitable for observing the transition from initial cardiomyocyte hypertrophy to later cardiac remodeling and heart failure.

The evaluation of AAC model was based on the hemodynamic, morphometric and echocardiographic characteristics, which included (1) cardiac remodeling as reflected by increased LV/body weight ratio, collagen volume fraction, and wall thickness, and (2) cardiac dysfunction as indicated by impaired +dP/dtmax, −dP/dtmax, ejection fraction, and fractional shortening (Tables 1–4).

The 8-week treatment improved both the perivascular and the interstitial collagen volume fraction in the AAC rat model. In contrast, the improvement in perivascular and interstitial collagen volume fraction was relatively weak following 2 weeks of treatment (Tables 3 and 4). We found that although MG132 remarkably decreased cardiac hypertrophy, LV remodeling and significantly improved cardiac diastolic function, cardiac systolic function indicated by +dP/dtmax, FS, LVSP, and EF was similar between MG132- and vehicle-treated AAC rats by 2 weeks. This indicated that the compensatory cardiac hypertrophy was not required to maintain cardiac function at the early phase of pressure overload, on the contrary, it decreased cardiac diastolic function. However, 8 weeks of treatment with MG132 not only improved cardiac diastolic function but also cardiac systolic function as well as effectively attenuated ventricular hypertrophy. These results suggested a potential role for proteasome inhibition as a new chronic therapeutic strategy for prevention of cardiac remodeling and heart failure caused by pressure overload.

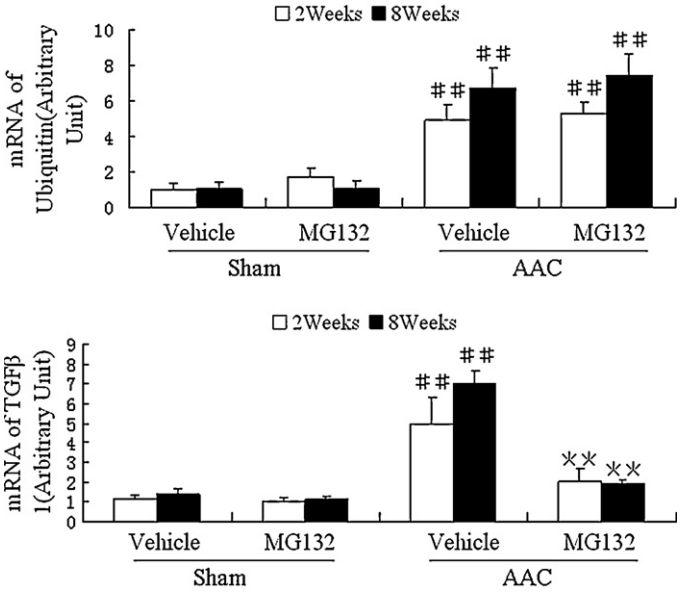

Fig. 2. Effects of MG132 on ubiquitin and TGFβ1 mRNA expression after 2 or 8 weeks of treatment. (A) Relative level of ubiquitin mRNA expression. (B) Relative level of TGFβ1 mRNA expression. $^{\#\#}P<0.01$ *vs.* vehicle-treated sham group, $^{**}P<0.01$ *vs.* vehicle-treated AAC group.

No significant changes in carotid artery pressure (data not shown) and LVSP (Tables 3 and 4) following 2 or 8 weeks of treatment with MG132 were observed, indicating that the protective effects of MG132 on AAC rats was not due to altering blood pressure.

Although most experimental studies have suggested that acute proteasome inhibition can suppress cardiac hypertrophy, it remains controversial whether chronic treatment has beneficial effects on cardiac remodeling and dysfunction since chronic proteasome inhibition for myeloma treatment caused heart failure in several clinic cases [32]. Dramatic down-regulation of cardiac proteasome activities was also observed in end-stage heart failure patients [6]. It also remains unclear whether this down-regulation is the result or the compensatory mechanism of the progression of the disease. We investigated the effects of proteasome inhibition from the initiation of pressure overload to decompensated heart failure and found that chronic proteasome inhibition (at least 8 weeks) attenuated cardiac fibrosis and dysfunction. We also found that proteasome activities were increased in AAC rats with heart failure. However, whether they decrease with the progression of heart failure and then the effects of proteasome inhibition require further study. In addition, the difficulties in timely, moderately and effectively inhibiting the proteasome and a poor understanding of the mechanism underlying the effects of proteasome inhibition on the heart also arouse the controversy [13].

In order to better understand the beneficial effects of MG132 on ventricular remodeling and cardiac function due to pressure overload, we next focused on the NF-κB signaling pathways. We found that expression of NFκB-p65, TGFβ1, and Smad2 and the activity of NF-κB in LV was significantly higher in the Vehicle/AAC treated group, as compared with the Vehicle/Sham group. However the protein expression levels of IκB-α decreased significantly in the Vehicle/AAC group, as compared with the Vehicle/Sham group. In MG132-treated rats the expression of NFκB-p65, TGFβ1, and Smad2 and the activity of NF-κB were down-regulated, while IκB-α protein was up-regulated, as compared with Vehicle-treated AAC rats. These results indicated that the proteasome inhibitor, MG132, prevented degradation of IκB-α and then inhibited activation of NF-κB; these findings were also in agreement with the previous studies [10]. Considering the previous studies [16–20] and our results, we hypothesized that MG132 could significantly down-regulate the expression of TGFβ1 and Smad2 through inhibition of NF-κB activity.

Since accumulating evidence showed that NF-κB and TGFβ1/Smad2 played a key role in cardiac remodeling in the pressure-overloaded heart, MG132 may act to attenuate ventricular remodeling and improve cardiac function through the inhibition of NF-κB and TGFβ1 signaling pathways. Although we did not use a specific antagonist of NF-κB or undertake gene knockout for

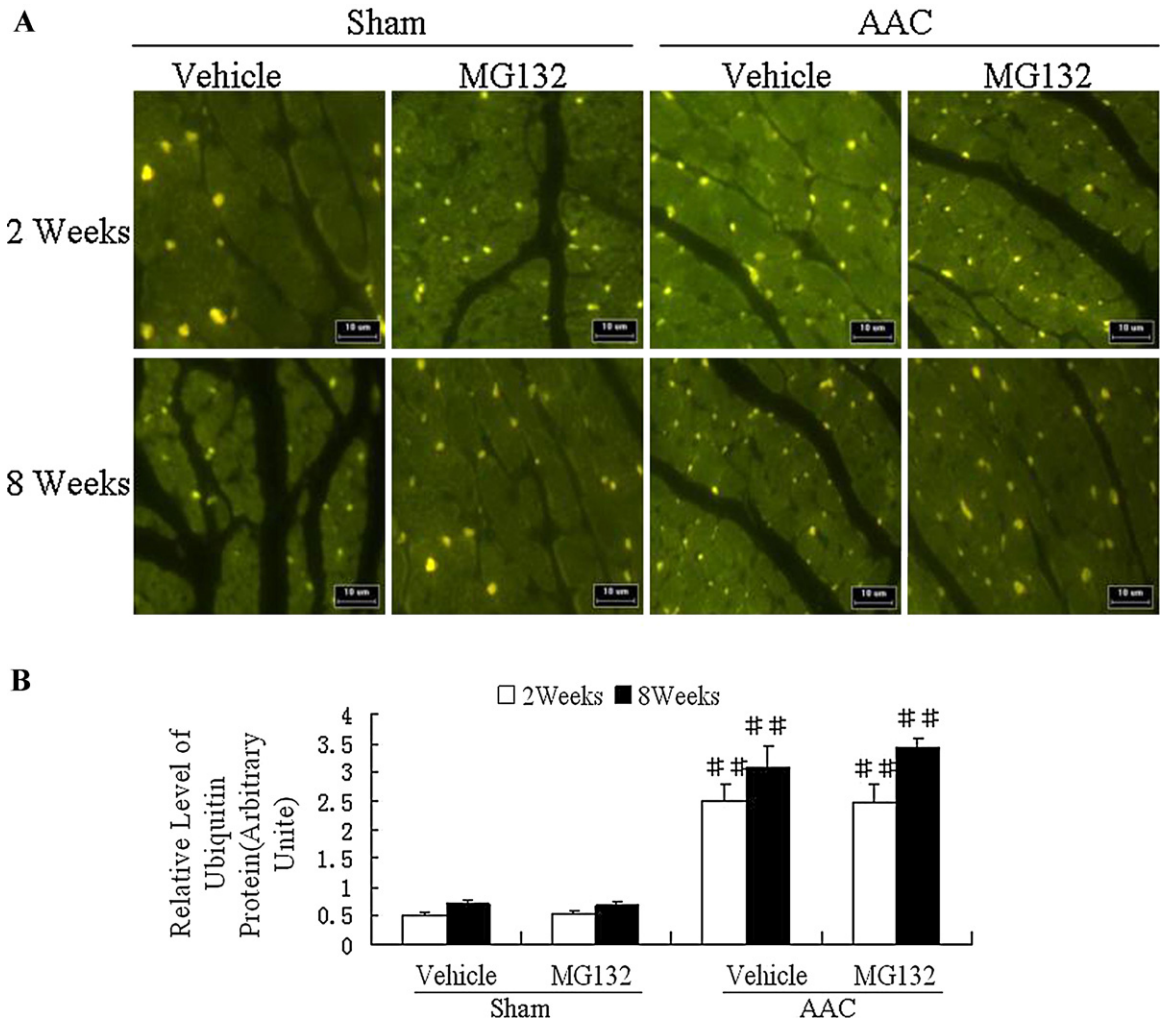

Fig. 3. Effects of MG132 on the expression of total ubiquitin proteins detected by immunofluorescence. (A) Representative Immunofluorescence image high magnification (400×) of ubiquitin protein of left ventricles from different groups, bar, 10 μm. (B) Relative level of ubiquitin protein. $^{\#\#}P < 0.01$ *vs.* vehicle-treated sham group.

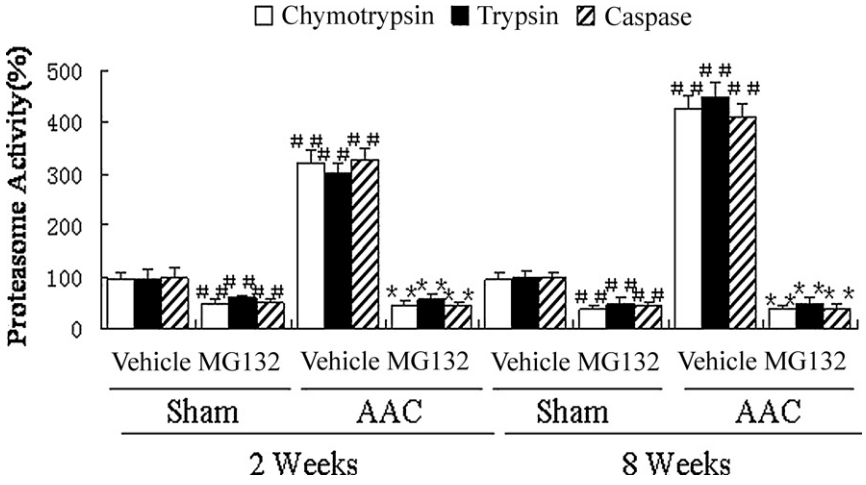

Fig. 4. Effects of MG132 on the proteasome activity. (A) Effect of MG132 on the proteolytic activity of the 26S proteasome after 2 weeks of treatment. (B) Effect of MG132 on the proteolytic activity of the 26S proteasome after 8 weeks of treatment. Proteasome activity is expressed as percent activity of the Vehicle/Sham group. $^{\#\#}P < 0.01$ *vs.* vehicle-treated sham group, $^{**}P < 0.01$ *vs.* vehicle-treated AAC group.

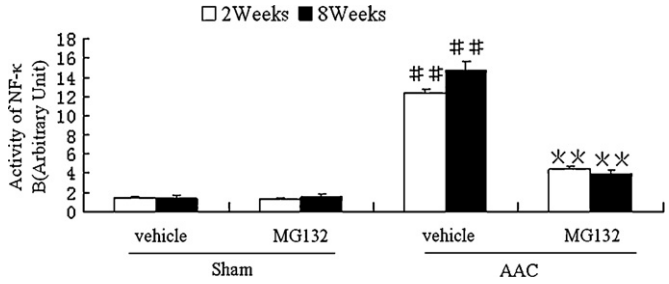

Fig. 5. Effects of MG132 on activity of NF-κB measured by ELISA. $^{\#\#}P < 0.01$ *vs.* vehicle-treated sham group, $^{**}P < 0.01$ *vs.* vehicle-treated AAC group.

NF-κB, we did measure the changes of NF-κB activity in different groups and observed MG132 was able to suppress the expression of TGFβ1 and Smad2 via inhibition of NF-κB.

However, it remains unclear why TGFβ1 and Smad2 were not markedly depressed and IκB-α was not up-regulated in the MG132/Sham group in which proteasome activity was decreased significantly. We found that MG-132 treatment had a significant but relatively weak effect on proteasome activity in the MG132/Sham group, but completely prevented the induction of proteasome activity in the MG132/AAC group (Fig. 4). It is possible that the subunit composition of the proteasome is altered during pressure-overload induced cardiac remodeling resulting in a different susceptibility to MG-132 inhibition [12]. In addition, an appropriate NF-κB activity is needed for the body, which may be through some kind of compensatory mechanism to balance or offset the inhibitory effects of MG132 on IκB-α degradation. A previous study on cancer has shown that MG132 selectively inhibited NF-κB activity in tumor cells without affecting NF-κB activity in normal surrounding tissue cells [33]. Thus, weak inhibition of the proteasome and so-called body self- regulation may explain why MG132 had no effects on IκB-α, NF-κB, TGFβ1 and Smad2 in sham-operated rats.

We know that NF-κB is a key transcription factor involved in the regulation of diverse biological phenomena, including inflammation, immune, apoptosis, cell maturation, cell proliferation and the cellular responses to stress, NF-κB is not only a major mediator of cytokine effects in the heart but also a signaling integrator, thus it acts as a key regulator of cardiac gene expression programs and is implicated in the regulation of downstream of multiple signal transduction cascades in a variety of physiological and pathophysiological states [34]. In the previous study, we found that long-term treatment with MG132 attenuated pressure overload-induced cardiac hypertrophy through down regulation of ERK1/2 and JNK1 signaling pathways which are both classical MAPK pathways [14]. NF-κB and MAPK signaling pathways can interact with each other through biochemical cross-talk [35]. Craig et al. [36] found p38 can activate NF-κB through activating IκB kinase, while Lin et al. [37] demonstrated that the inhibitor for JNK (i.e., SP600125) attenuated the TNF-α-induced NF-κB activation. Our studies also found that there was a consistent trend in alterations of NF-κB and MAPK signaling pathways in the pressure overload heart with or without MG132 administration. In view of these studies, we speculate that MG132 suppressed NF-κB activity in the pressure overload heart directly by inhibition of IκB-α degradation and indirectly through down regulation of MAPKs, although the precise mechanisms require further investigation.

Furthermore, our results showed that the level of angiotensin II in plasma and myocardium was significantly higher in the AAC rats than in the Sham-treated rats. It is well-established that angiotensin II plays a critical role in the development of ventricular remodeling and heart failure. Some studies have demonstrated that angiotensin II is able to activate the UPS in skeletal muscle [38,39]. Although little is known about the effects of angiotensin II on the cardiac proteasome, there is a possibility that the beneficial

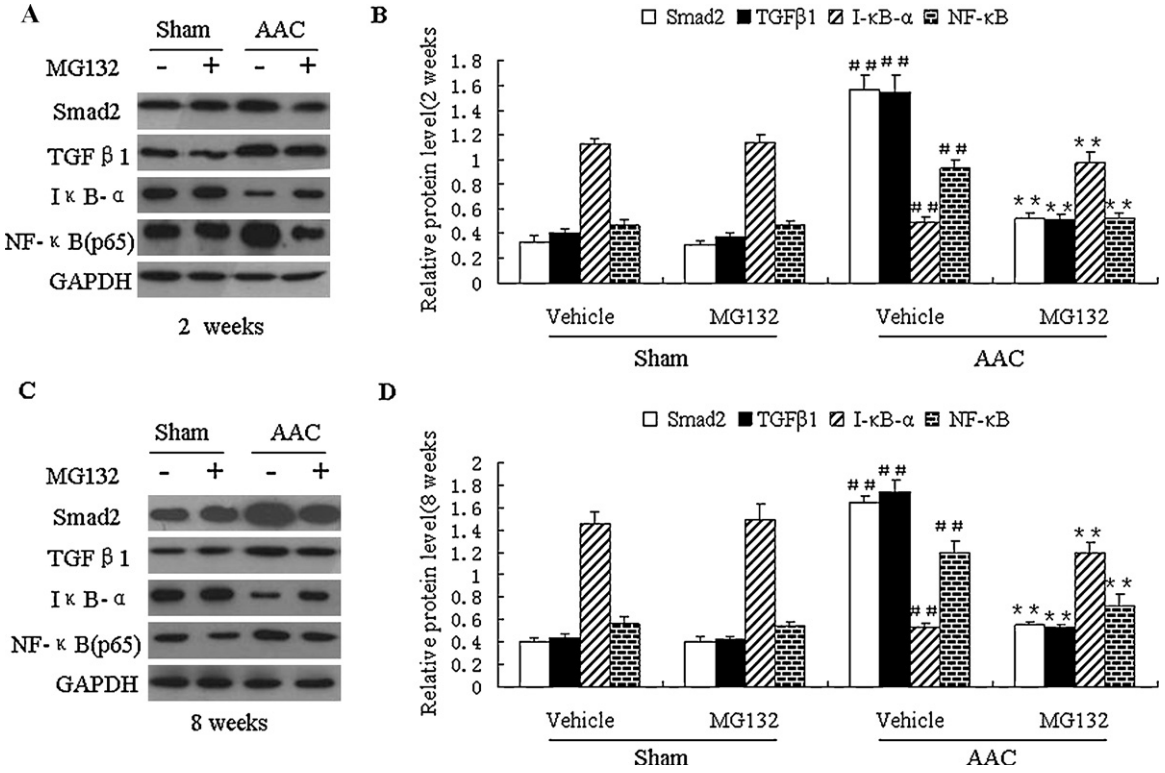

Fig. 6. Effects of MG132 on NF-κB signaling pathway-related protein expression. Western blot for Smad2, TGFβ1, IκB-α and NF-κB (p65) protein after 2 weeks (A) or 8 weeks (C) of treatment with MG132. Densitometric analysis of relative levels of Smad2, TGFβ1, IκB-α and NF-κB (p65) protein (band density of the protein of interest/GAPDH band density) after 2 weeks (B) or 8 weeks (D) of treatment with MG132. $^{\#\#}P < 0.01$ *vs.* vehicle-treated sham group, $^{**}P < 0.01$ *vs.* vehicle-treated AAC group.

effects of MG132 on ventricular remodeling and heart failure occurs by MG132 blocking the downstream signaling pathway of angiotensin II, in addition to inhibiting NF-κB. This possibility is very interesting and worthy of further investigation.

In summary, the present study showed that the activity of proteasomes within the LV myocardium continuously increased both in the early and in the late stages of pressure overload (Fig. 4). Compensatory cardiac hypertrophy is dispensable in progression towards heart failure. The pressure-overloaded heart can benefit from both short- and long-term proteasome inhibition treatments by MG132. Its inhibiting effects on ventricular remodeling may be mediated through NF-κB and MAPK signaling pathways. Therefore, inhibition of proteasome activity with MG132 may represent a novel therapeutic choice for preventing hypertensive cardiac remodeling.

Acknowledgements

This work was supported by the National Natural Science Foundation of China [Grants 30971260]; and the Natural Science Foundation of Guangdong Province [Grants 8251008901000013].

References

[1] Cuspidi C, Ciulla M, Zanchetti A. Hypertensive myocardial fibrosis. Nephrol Dial Transplant 2006;21(1):20–3.
[2] Weber KT, Sun Y, Guarda E, Katwa LC, Ratajska A, Cleutjens JP, et al. Myocardial fibrosis in hypertensive heart disease: an overview of potential regulatory mechanisms. Eur Heart J 1995;16(Suppl. C):24–8.
[3] Jessup M, Brozena S. Heart failure. N Engl J Med 2003;348:2007–18.
[4] Birks EJ, Latif N, Enesa K, Folkvang T, Luong le A, Sarathchandra P, et al. Elevated p53 expression is associated with dysregulation of the ubiquitin-proteasome system in dilated cardiomyopathy. Cardiovasc Res 2008;79:472–80.
[5] Hein S, Arnon E, Kostin S, Schonburg M, Elsasser A, Polyakova V, et al. Progression from compensated hypertrophy to failure in the pressure-overloaded human heart: structural deterioration and compensatory mechanisms. Circulation 2003;107:984–91.
[6] Tsukamoto O, Minamino T, Okada K, Shintani Y, Takashima S, Kato H, et al. Depression of proteasome activities during the progression of cardiac dysfunction in pressure-overloaded heart of mice. Biochem Biophys Res Commun 2006;340:1125–33.
[7] Weekes J, Morrison K, Mullen A, Wait R, Barton P, Dunn MJ. Hyperubiquitination of proteins in dilated cardiomyopathy. Proteomics 2003;3:208–16.
[8] Depre C, Wang Q, Yan L, Hedhli N, Peter P, Chen L, et al. Activation of the cardiac proteasome during pressure overload promotes ventricular hypertrophy. Circulation 2006;114(17):1796–8.
[9] Hedhli N, Lizano P, Hong C, Fritzky LF, Dhar SK, Liu H, et al. Proteasome inhibition decreases cardiac remodeling after initiation of pressure overload. Am J Physiol Heart Circ Physiol 2008;295:H1385–93.
[10] Hedhli N, Lizano P, Hong C, Fritzky LF, Dhar SK, Liu H, et al. 4-Hydroxy-2-nonenal-mediated impairment of intracellular proteolysis during oxidative stress. Identification of proteasomes as target molecules. J Biol Chem 1999;274:23787–93.
[11] Meiners S, Dreger H, Fechner M, Bieler S, Rother W, Gunther C, et al. Suppression of cardiomyocyte hypertrophy by inhibition of the ubiquitin-proteasome system. Hypertension 2008;51:302–8.
[12] Christophe D, Powell SR, Wang X. The role of the ubiquitin-proteasome pathway in cardiovascular disease. Cardiovasc Res 2010;85:251–2.
[13] Su H, Wang X. The ubiquitin-proteasome system in cardiac proteinopathy: a quality control perspective. Cardiovasc Res 2010;85:253–62.
[14] Chen BL, Ma YD, Meng RS, Xiong ZJ, Zhang CX, Chen GQ, et al. MG132, a proteasome inhibitor, attenuates pressure-overload-induced cardiac hypertrophy in rats by modulation of mitogen-activated protein kinase signals. Acta Biochim Biophys Sin 2010;42(4):253–8.
[15] Meiners S, Hocher B, Weller A, Laule M, Stangl V, Guenther C, et al. Down-regulation of matrix metalloproteinases and collagens and suppression of cardiac fibrosis by inhibition of the proteasome. Hypertension 2004;44:471–7.
[16] Hautmann MB, Adam PJ, Owens GK. Similarities and differences in smooth muscle alpha-actin induction by TGF-beta in smooth muscle versus non-smooth muscle cells. Arterioscler Thromb Vasc Biol 1999;19(9):2049–58.
[17] Sun Y, Zhang J, Zhang JQ, Ramires FJ. Local angiotensin II and transforming growth factor-beta1 in renal fibrosis of rats. Hypertension 2000;35(5):1078–84.
[18] Tomasek JJ, Gabbiani G, Hinz B, Chaponnier C, Brown RA. Myofibroblasts and mechano-regulation of connective tissue remodeling. Nat Rev Mol Cell Biol 2002;3(5):349–63.
[19] Villarreal FJ, Lee AA, Dillmann WH, Giordano FJ. Adenovirus-mediated overexpression of human transforming growth factor-beta 1 in rat cardiac fibroblasts, myocytes and smooth muscle cells. J Mol Cell Cardiol 1996;28(4):735–42.
[20] Seo D, Hare JM. The transforming growth factor-beta/Smad3 pathway: coming of age as a key participant in cardiac remodeling. Circulation 2007;116(19):2096–8.
[21] Lan Y, Zhou Q, Wu ZL. NF-kappa B involved in transcription enhancement of TGF-beta 1 induced by Ox-LDL in rat mesangial cells. Chin Med J 2004;117225–30.
[22] Shinozaki S, Mashima H, Ohnishi H, Sugano K. IL-13 promotes the proliferation of rat pancreatic stellate cells through the suppression of NF-jB/TGF-b1 pathway. Biochem Biophys Res Commun 2010;393:61–5.
[23] Hedhli N, Pelat M, Depre C. Protein turnover in cardiac cell growth and survival. Cardiovasc Res 2005;68:186–96.
[24] Palombella VJ, Rando OJ, Goldberg AL, Maniatis T. The ubiquitin proteasome pathway is required for processing the NF-kappa B1 precursor protein and the activation of NF-kappa B. Cell 1994;78:773–85.
[25] Ulla J, Paukkeri EL, Moilanen E. Compounds that increase or mimic cyclic adenosine monophosphate enhance tristetraprolin degradation in lipopolysaccharide-treated murine J774 macrophages. J Pharmacol Exp Ther 2008;326:514–22.
[26] Dupont-Versteegden EE, Fluckey JD, Knox M, Gaddy D, Peterson CA. Effect of flywheel-based resistance exercise on processes contributing to muscle atrophy during unloading in adult rats. J Appl Physiol 2006;101:202–12.
[27] Meiners S, Heyken D, Weller A, Ludwig A, Stangl K, Kloetzel PM, et al. Inhibition of proteasome activity induces concerted expression of proteasome genes and de novo formation of Mammalian proteasomes. J Biol Chem 2003;278:21517–25.
[28] Okada K, Wangpoengtrakul C, Osawa T, Toyokuni S, Tanaka K, Uchida K. 4-Hydroxy-2-nonenal-mediated impairment of intracellular proteolysis during oxidative stress. Identification of proteasomes as target molecules. J Biol Chem 1999;274:23787–93.
[29] Qiu JH, Asai A, Chi S, Saito N, Hamada H, Kirino T. Proteasome inhibitors induce cytochrome c-caspase-3-like protease mediated apoptosis in cultured cortical neurons. J Neurosci 2000;20:259–65.
[30] Peng Y, Popović ZB, Sopko N, Drinko J, Zhang Z, Thomas JD, et al. Speckle tracking echocardiography in the assessment of mouse models of cardiac dysfunction. Am J Physiol 2009;297:H811–20.
[31] Shizukuda Y, Buttrick PM, Geenen DL, Borczuk AC, Kitsis RN, Sonnenblick EH, et al. β-Adrenergic stimulation causes cardiocyte apoptosis: influence of tachycardia and hypertrophy. Am J Physiol 1998;275:H961–8.
[32] Yeh ET, Bickford CL. Cardiovascular complications of cancer therapy: incidence, pathogenesis, diagnosis, and management. J Am Coll Cardiol 2009;53(24):2231–47.
[33] Graham W, Kris G, Yong X, Mahesh K, Clair William ST. Selectively enhanced radiation sensitivity in prostate cancer cells associated with proteasome inhibition. Oncol Rep 2005;15:1287–91.
[34] Jones WK, Brown M, Ren X, He S, McGuinness M. NF-kappaB as an integrator of diverse signaling pathways: the heart of myocardial signaling? Cardiovasc Toxicol 2003;3(3):229–54.
[35] Mercurio F, Zhu H, Murray BW, Shevchenko A, Bennett BL, Li J, et al. IKK-1 and IKK-2: cytokine-activated IkappaB kinases essential for NF-kappaB activation. Science 1997;278(5339):860–6.
[36] Craig R, Larkin A, Mingo AM, Thuerauf DJ, Andrews C, McDonough PM, et al. p38 MAPK and NF-kappa B collaborate to induce interleukin-6 gene expression and release. Evidence for a cytoprotective autocrine signaling pathway in a cardiac myocyte model system. J Biol Chem 2000;275(31):23814–2.
[37] Lin CW, Chen LJ, Lee PL, Lee CI, Lin JC, Chiu JJ. The inhibition of TNF-alpha-induced E-selectin expression in endothelial cells via the JNK/NF-kappaB pathways by highly N-acetylated chitooligosaccharides. Biomaterials 2007;28(7):1355–66.
[38] Sanders PM, Russell ST, Tisdale MJ. Angiotensin II directly induces muscle protein catabolism through the ubiquitin-proteasome proteolytic pathway and may play a role in cancer cachexia. Br J Cancer 2005;93:425–34.
[39] Song YH, Li Y, Du J, Mitch WE, Rosenthal N, Delafontaine P. Muscle-specific expression of IGF-1 blocks angiotensin II-induced skeletal muscle wasting. J Clin Invest 2005;115:451–8.